

## Weakening of North Indian SST Gradients and the Monsoon Rainfall in India and the Sahel

CHUL EDDY CHUNG AND V. RAMANATHAN

*Center for Clouds, Chemistry, and Climate, Scripps Institution of Oceanography, La Jolla, California*

(Manuscript received 19 September 2005, in final form 11 January 2006)

### ABSTRACT

Sea surface temperatures (SSTs) in the equatorial Indian Ocean have warmed by about 0.6–0.8 K since the 1950s, accompanied by very little warming or even a slight cooling trend over the northern Indian Ocean (NIO). It is reported that this differential trend has resulted in a substantial weakening of the meridional SST gradient from the equatorial region to the South Asian coast during summer, to the extent that the gradient has nearly vanished recently. Based on simulations with the Community Climate Model Version 3 (CCM3), it is shown that the summertime weakening in the SST gradient weakens the monsoon circulation, resulting in less monsoon rainfall over India and excess rainfall in sub-Saharan Africa. The observed trend in SST is decomposed into a hypothetical uniform warming and a reduction in the meridional gradient. The uniform warming of the tropical Indian Ocean in the authors' simulations increases the Indian summer monsoon rainfall by 1–2 mm day<sup>-1</sup>, which is opposed by a larger drying tendency due to the weakening of the SST gradient. The net effect is to decrease the Indian monsoon rainfall, while preventing the sub-Saharan region from becoming too dry. Published coupled ocean–atmosphere model simulations are used to describe the competing effects of the anthropogenic radiative forcing due to greenhouse gases and the anthropogenic South Asian aerosols on the observed SST gradient and the monsoon rainfall.

### 1. Introduction

The Indian subcontinent and the Sahel region in Africa have a rainy season in boreal summer. These areas witnessed generally negative summer rainfall anomalies since the 1950s. Hulme (1996) reported a significant desiccation trend in the Sahel region of sub-Saharan Africa in the latter half of the twentieth century. Hoerling et al. (2006) estimated the Sahelian rainfall reduction to be around 35% since 1950. The drying trend in sub-Saharan Africa was most conspicuous and pronounced from 1950 to 1985, and since 1985 this area has been slowly recovering. Giannini et al. (2003) demonstrated with an atmospheric general circulation model (AGCM) that the Sahel drying trend can be well simulated by the observed trends in the global sea surface temperatures (SSTs). They concluded that the warming trends in the equatorial Atlantic and Indian Oceans were the likely trigger for the decrease in Sahelian rain-

fall. This finding was further refined by Hoerling et al. (2006) who showed (again with AGCMs) that the Atlantic SST trend was the primary contributor to the Sahelian drought. The cause of the Atlantic SST trends was taken up by Rotstayn and Lohmann (2002), who proposed that the Northern Hemisphere sulfate aerosols had preferentially cooled the northern tropical Atlantic compared with the southern Atlantic, which was not subject to as much aerosol pollution. Based on experiments with an AGCM coupled to a slab ocean model, they hypothesized that this relative cooling of the North Atlantic led to a southward shift of the intertropical convergence zone (ITCZ), which in turn led to the Sahelian drought. These and other studies (see the references in Hoerling et al. and Giannini et al.) have clearly established SST variability as the major forcing term for the rainfall trends in Africa.

The North African monsoon is also known to connect with the South Asian monsoon. Webster and Fasullo (2003) explain that South Asian monsoon circulation has a profound effect on North African monsoon through the mid- and upper troposphere easterly jets, which extend all the way from the eastern Indian Ocean/South Asian region to as far west as the west

---

*Corresponding author address:* C. E. Chung, Center for Atmospheric Sciences, Scripps Institution of Oceanography, Mail Code 0221, 9500 Gilman Drive, La Jolla, CA 92093.  
E-mail: cchung@fiji.ucsd.edu

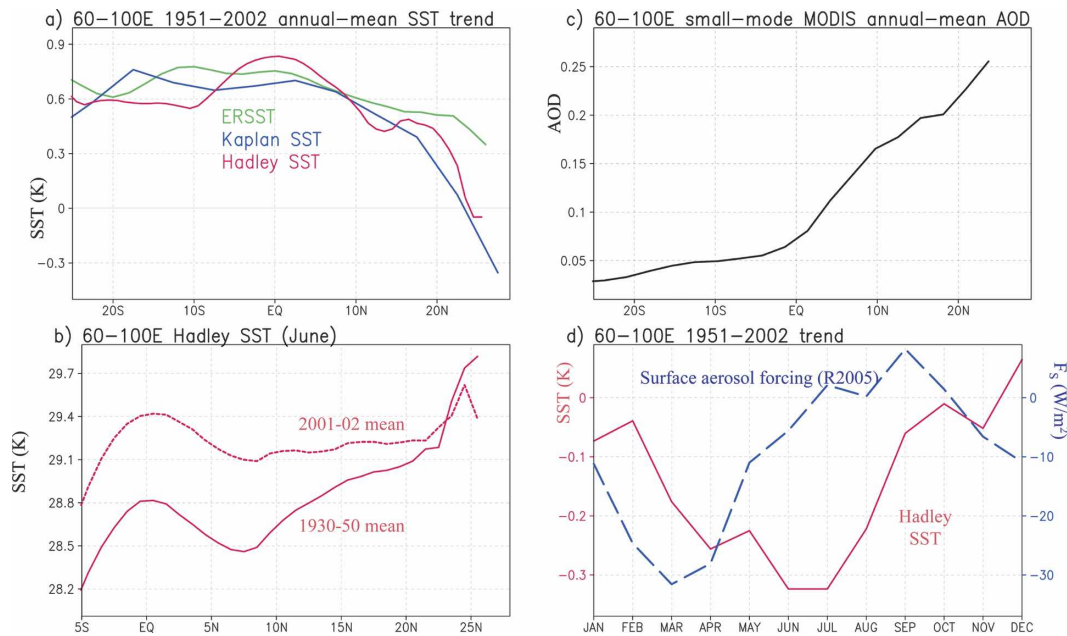


FIG. 1. Observed meridional SST trends, SSTs, aerosol distribution, and forcing and trends in meridional SST gradients for the Indian Ocean. (a) The 1951–2002 trend in annual-mean SST from three datasets: National Oceanic and Atmospheric Administration (NOAA) Extended Reconstructed (ER) SST (Smith and Reynolds 2004), Kaplan SST (Kaplan et al. 1998), and Hadley Centre SST (Rayner et al. 2003). The “trend” denotes the change in SST for the 52 yr, i.e.,  $\text{K (52 yr)}^{-1}$ . (b) Hadley Centre June SST for two periods. (c) Small-mode AOD over the Indian Ocean derived from the satellite MODIS instrument (3-yr mean over 2001–03). (d) Monthly variation in the 1951–2002 trend [ $\text{K (52 yr)}^{-1}$ ] in the meridional Hadley SST gradient and in the simulated surface solar radiation meridional gradient in R2005. The meridional gradient is computed by  $5^{\circ}$ – $25^{\circ}\text{N}$  and  $-20^{\circ}\text{S}$ – $0^{\circ}$  mean in (d). The 1951–2002 trend in the simulated surface radiation is essentially the anthropogenic aerosol radiative forcing at the surface in this basin. All of the trends in this and subsequent figures are linear fits over the period and are displayed in units of change over the entire period length (in this figure, 52 yr, i.e., from 1951 to 2002). The trend unit “ $52 \text{ yr}^{-1}$ ” is omitted.

coast of North Africa. The implication is that variations in the South Asian monsoon can influence North African rainfall variations. The monsoon rainfall over India has decreased by about 5%–8% since the 1950s (Ramanathan et al. 2005, hereafter R2005). Superposed on this longer-term change are rainfall variations on intraseasonal, interannual, and interdecadal time scales (Webster et al. 1998; Sikka 2003).

Various sources of SST data (Smith and Reynolds 2004; Kaplan et al. 1998; Rayner et al. 2003) reveal that the tropical Indian Ocean, particularly the equatorial portion, has warmed substantially since the 1950s (Fig. 1a). This warming trend is at odds with the decreasing summer rainfall trend over India (Fig. 2a) since modeling studies show that the greenhouse gas (GHG) forcing induces a uniform warming of the tropical Indian Ocean, which in turn leads to intensified evaporation from the Indian Ocean, enhanced moisture, and increased monsoon rainfall in India (Meehl et al. 1993; Meehl and Arblaster 2003; Douville et al. 2000; May

2002; R2005). R2005 considered the effects of both the GHGs and absorbing South Asian anthropogenic aerosols (also referred to as brown haze) in a coupled ocean–atmosphere GCM (OAGCM). Their OAGCM simulations showed that the increase in GHGs led to a uniform warming of the tropical Indian Ocean by about 0.5 K, while the negative aerosol forcing (a cooling effect) masked the GHG warming in the northern Indian Ocean (NIO) and weakened the meridional SST gradient in summer. R2005 concluded that a large increase in aerosol emission in South Asia since the 1930s may help explain the observed decrease in the Indian monsoon rainfall.

These earlier studies provide the motivation for examining the long-term trends in meridional SST gradients in the tropical Indian Ocean and identifying the specific role of the SST trends in the monsoon rainfall. We specifically focus on the period from 1950 to 2002 when the SST data over the Indian Ocean are more reliable. The present study, since it focuses on observed

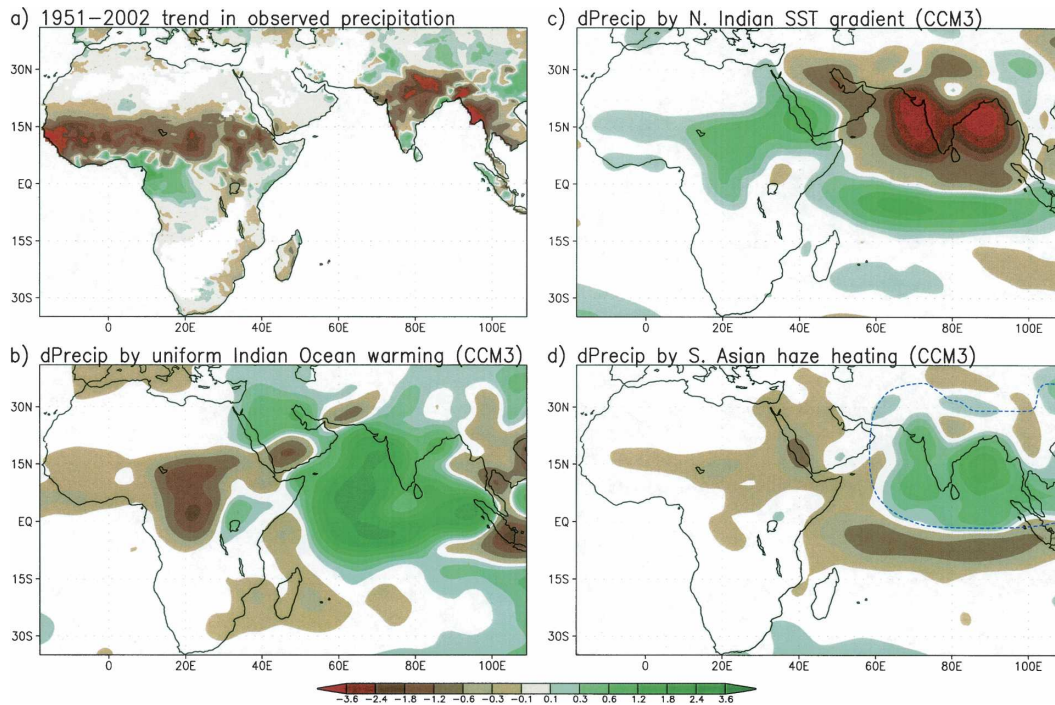


FIG. 2. Precipitation trend or change averaged from June to September (in units of  $\text{mm day}^{-1}$ ). (a) The 1951–2002 trend in CRU precipitation (Mitchell and Jones 2005); note that no shading indicates lack of data. (b) Simulated precipitation change due to the hypothetical uniform warming in the northern Indian Ocean (UNIF – CONT); see section 3 and Table 1 for details. (c) Simulated precipitation change due to the meridional SST gradient modification in the Indian Ocean (IND – UNIF). (d) Simulated precipitation change due to the atmospheric heating by the South Asian haze (HEAT1 – CONT); the dash circle denotes the area where the haze heating was inserted in the CCM3. In (b)–(d), no shading indicates changes less than  $0.1 \text{ mm day}^{-1}$ . The simulated precipitation change in (b)–(d) has an uncertainty of about 0.2 over the central Africa and about 0.4 over India at the 95% confidence level; uncertainty is due to a limited number of ensemble runs.

SST trends and their influence on monsoon rainfall, is in contrast with that of R2005, which relied on coupled ocean–atmosphere model simulations.

## 2. Trends in meridional SST gradients

The relative cooling of the northern Indian Ocean, compared with the warming trend of the equatorial Indian Ocean, is indeed evident in many different SST datasets (Fig. 1a). Climatologically, the Indian Ocean is warmest around the equator and colder away from it. During boreal late spring and summer, however, the warmest waters extend from the equator to the northern Arabia Sea and Bay of Bengal where the SSTs exceed equatorial SSTs, enabling a full development of the Indian monsoon (Fig. 1b; see the 1930–50 mean SSTs). Various SST observations all show a large warming trend in the equatorial zone since the 1950s and a much smaller warming trend (or even a slight cooling trend) north of it, thereby modifying the north–south SST gradient (Fig. 1a). Annually, the Hadley SST

dataset (Rayner et al. 2003) shows about  $0.6\text{--}0.8\text{ K}$  warming around the equator in the last 50 yr, but very little warming in the Bay of Bengal and the Arabian Sea. This heterogeneous warming has weakened the meridional SST gradient northward from the equator in late spring and summer sufficiently that the June SST gradient has nearly vanished in the recent years (Fig. 1b). For June, the  $60^{\circ}\text{--}100^{\circ}\text{E}$  SST difference between the equator and  $25^{\circ}\text{N}$  was about  $1 \text{ K}$  in the early twentieth century, but this difference was almost zero in 2001 and 2002 (Fig. 1b). The meridional SST gradient trend has a strong seasonal dependence (Fig. 1d). The 1951–2002 trend in the meridional SST gradient (SST difference between  $20^{\circ}\text{S}$ –equator and  $5^{\circ}\text{--}25^{\circ}\text{N}$ ) is most negative in summer.

How has the observed weakening trend in the NIO\_SST gradient affected the monsoon circulation and regional rainfall over India and the Sahel? The present study is largely motivated by this question. During late spring and summer, the surface pressure over the ocean south of the equator is higher ( $>1015 \text{ mb}$ )

TABLE 1. List of all the numerical experiments in this study. All the experiments were conducted using the NCAR/CCM3 with yearly repeating SSTs. The differences between experiments lie in solar radiation perturbation (due to South Asian haze) and/or the prescribed SSTs.

Acronym	Prescribed SSTs	Solar radiation
CONT	Climatology	Background
GLOBE	1951–2002 trend imposed globally	Background
IND	1951–2002 trend imposed in the Indian Ocean	Background
UNIF	Hypothetical uniform warming imposed in the northern Indian Ocean	Background
HEAT1	Climatology	South Asian haze effects at the 1995–2004 level
HEAT2	Climatology	Hypothetically stronger South Asian haze effects on the solar radiation

than that over the warmer NIO ( $<1005$  mb) (Webster and Fasullo 2003). This cross-equatorial pressure gradient drives the southwesterly monsoon flow that carries moisture from the ocean toward South Asia. Because deep convection preferentially occurs over warmer water, SST gradients play an important role in creating the reverse pressure gradient (with higher pressure north of the equator) in the mid- and upper troposphere that maintains the upper-level monsoon outflow (Webster et al. 1998). Thus from a dynamical consideration a weakening of the SST gradients in the NIO can weaken the monsoon circulation, by weakening both the cross-equatorial (south to north) surface pressure gradient and north-to-south mid- and upper-troposphere pressure gradient. Since one branch of the outflow from South Asia forms the so-called easterly jet, which descends over the North African region (Webster and Fasullo 2003), a weakening of the monsoon circulation can in turn modulate African rainfall.

In addition, we will consider an important follow-on question regarding the connection between the brown haze (i.e., anthropogenic aerosols), the meridional SST gradient, and the regional monsoon rainfall. Figure 1c shows the 2001–03 small-mode aerosol optical depth (AOD) derived from the Moderate Resolution Imaging Spectroradiometer (MODIS) instrument on board the *Terra* satellite (Kaufman et al. 2002). The small-mode AOD is the AOD of submicron-size particles and is a good indicator of anthropogenic aerosols as discussed by Kaufman et al. (2002). Furthermore, as shown by Indian Ocean Experiment (INDOEX) aircraft observations (Ramanathan et al. 2001), roughly 75% of the total AOD over the northern Indian Ocean is due to anthropogenic emissions from South and Southeast Asia. The small-mode AOD increases fivefold from about 0.05 south of the equator to about 0.25 north of  $20^{\circ}\text{N}$ , and it is this latitudinal AOD gradient that led to a strong latitudinal gradient aerosol radiative forcing at the surface, varying from about 0 to  $-5 \text{ W m}^{-2}$  south of the equator to about  $-20$  to  $-30 \text{ W m}^{-2}$  around  $20^{\circ}\text{N}$

over the Arabian Sea and Bay of Bengal. It is this gradient in the negative surface forcing (surface cooling) that led to the weakening in the NIO\_SST gradient in R2005's simulations. Note, however, the aerosol forcing has a strong seasonal dependence as shown in Fig. 1d. The peak in the negative forcing leads the peak in the negative SST gradient trend by a few months. The thermal inertia of the ocean can account for the few months delay between the aerosol forcing and the SST response.

### 3. Numerical experiments

A series of numerical experiments were conducted with the National Center for Atmospheric Research Community Climate Model Version 3 (NCAR/CCM3) (Kiehl et al. 1998) at the T42/L18 resolution. The CCM3 includes an interactive land surface model (Bonan 1996) and uses prescribed SSTs. Control simulation (CONT) is conducted with climatological SSTs. Experiment simulations are run by superposing the observed SST changes on the climatological SSTs. In some of the numerical experiments we also include the haze radiative forcing. See Table 1 for the list of all the experiments conducted for this study. For each experiment, we perform 10 ensemble member simulations. For each of 10 ensemble simulations, we run the model for 6 yr; the only difference between the 10 ensemble simulations is that each is initialized with different atmospheric conditions. The model was found to equilibrate to the prescribed boundary conditions (SSTs or aerosol radiative forcing) in less than one year. After discarding the first year, the ten 5-yr simulations were averaged, yielding a 50-yr average sample for each of the few experiments reported here.

As for imposing the observed SST changes, we took the observed global SST from the Hadley Centre (Rayner et al. 2003) and calculated the trend for each month from 1951 to 2002. The trend is in units of  $\text{K (52 yr)}^{-1}$  or simply  $\text{K}$ . The trend for each oceanic grid



was added globally to the climatological SST of the CCM3 in the first experiment. In the second experiment, the observed 1951 to 2002 SST trend was imposed only for the northern Indian Ocean; the imposed SST changes in the southern Indian Ocean were brought to be zero linearly from 15° to 30°S for a smooth transition (experiment IND; Table 1). The third experiment uses the same SSTs except that the imposed northern Indian SST changes were flattened to the observed trend over the equatorial Indian Ocean, removing the SST gradient change therein (experiment UNIF). This experiment with uniform SST changes over the NIO uses the SST changes we would expect from solely the GHGs forcing. The tropospheric climate change by greenhouse gas concentration increase is mostly through the ocean warming (Ramanathan 1981), and so the uniform warming simulation (UNIF) essentially captures the monsoonal effects of the greenhouse gas increase.

Since the aerosol forcing is large and it has increased significantly during the period of interest, we did another experiment to quantify its role in the rainfall trends. The brown haze in South Asia and the nearby ocean has a lot of black carbon (soot) component and thus absorbs the solar radiation effectively (Ramanathan et al. 2001). The radiative forcing of this absorbing haze, other than its indirect effect through the SST gradient change, consists of a large heating of the lower atmosphere (because of soot absorption of the solar radiation) and a comparably large reduction in the surface solar radiation. Following Chung and Ramanathan (2003), we prescribe the atmospheric heating from the surface boundary layer to about 3 km, in addition to prescribing the surface solar radiation reduction (experiment HEAT1). In our CCM3 experiments where SSTs are held fixed, we find that the haze forcing impacts the simulated monsoon mainly through the atmosphere heating, and so we refer to the haze radiative forcing as haze heating here. As noted earlier, the NCAR/CCM3 includes an interactive surface model. Since the atmospheric solar absorption by the haze is accompanied by a corresponding decrease in surface solar radiation, the CCM3 land surface cools in the “haze heating” experiment. The magnitude of this cooling has been documented in the earlier studies of Chung et al. (2002) and Ramanathan et al. (2005). In spite of the land surface cooling the monsoon circulation response is dominated by the atmospheric haze heating, and hence we refer to this experiment as “haze heating” experiment. The seasonal variation of the imposed haze heating is the same as that in the numerical experiments of R2005.

#### 4. Connection between SST trends and monsoon rainfall trends

Figure 2a shows the observed 1951–2002 trend in June–September rainfall in units of millimeters per day change over the 52 yr. The rainfall observations were obtained from the Climatic Research Unit (CRU) archives (Mitchell and Jones 2005). Negative rainfall trends are widespread in the Sahel, India, and Southeast Asia. Figure 2b shows the simulated precipitation change by the Indian SST trend with the hypothetical uniform warming in the NIO as discussed in section 3 (UNIF – CONT). The uniform warming induces a substantial increase in monsoon rainfall ( $1.5 \text{ mm day}^{-1}$ ) over India, consistent with the earlier findings of Meehl and Arblaster (2003) that higher SSTs increase the Indian monsoon rainfall. The uniform warming also produces marginal drought in the Sahel through the tropical Africa. The statistical significance of the trends is discussed in the figure caption. In the next numerical experiment, we prescribe, as a function of calendar month, the actual observed SST trends in the Indian Ocean (IND). By subtracting the uniform-warming experiment results from this experiment with the observed Indian SST trend (IND – UNIF), the effects of the weakening trends in the NIO\_SST gradient have been isolated (Fig. 2c). Note that the southern Indian Ocean is treated in the same manner in both experiments. The most prominent feature of Fig. 2c is a large decrease in rainfall ( $-1$  to  $-2 \text{ mm day}^{-1}$ ) over India and a positive rainfall anomaly in sub-Saharan Africa. Analysis of the simulated wind change reveals that the weakening NIO\_SST gradient creates an overlying sinking motion over India and the NIO (red shaded region in Fig. 3a) with surface winds blowing from the subcontinent into the Arabia Sea, thus countering the climatological southwesterly monsoon winds. In short, the low-level monsoon circulation decreases in strength. Conservation of mass requires a corresponding weakening of the upper-level easterly outflow (easterly jet) toward Africa and the meridional outflow (part of the Hadley circulation) toward the equatorial ocean (Fig. 4). The net impact of the weakened circulation is surface wind convergence over northern Africa and the equatorial Indian Ocean, giving rise to rising motion and enhanced precipitation in these two regions (Fig. 3a). Effectively, the SST gradient reduction has shifted rain from India to sub-Saharan Africa and the equatorial Indian Ocean. The precipitation change caused by the weakening trends in the NIO\_SST gradient as in Fig. 2c also shows an increase over the equatorial Indian region. This feature is difficult to validate with observation because rainfall data over ocean are avail-

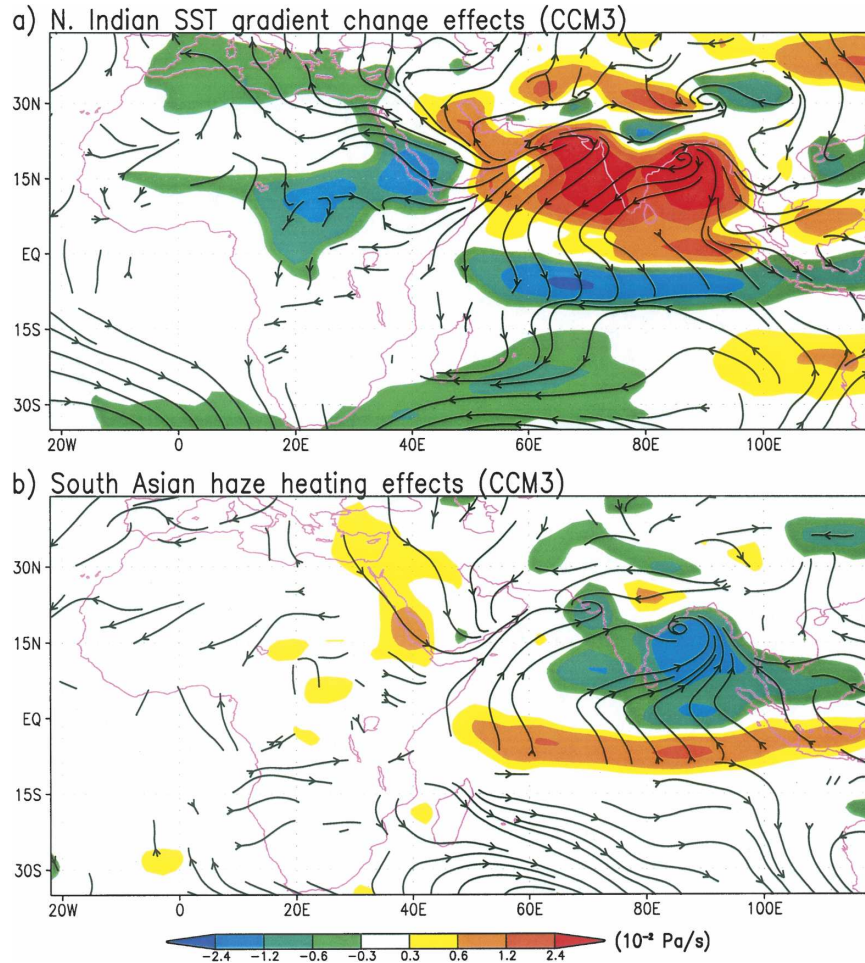


FIG. 3. Streamlines of the simulated surface wind change (June–September) by (a) north Indian SST gradient change (IND – UNIF) and (b) the South Asian haze radiative effects (HEAT1 – CONT). Shading displays the simulated vertical motion change over 500–300 hPa with red (blue) color associated with sinking (rising) motion. The vertical motion was calculated with pressure velocity  $\omega$  (in units of  $10^{-2} \text{ Pa s}^{-1}$ ).

able only for the recent decades. The 1975–2004 trends in outgoing longwave radiation (OLR) support a wetter trend over the equatorial Indian Ocean (Fig. 5).

In contrast, the experiment with the observed global SST trend (GLOBE – CONT) reduces precipitation over sub-Saharan Africa and produces less significant drought over India (not shown) than that due to the north Indian SST gradient change alone (Fig. 2c). Over India, the effects of the weakening trends in the NIO\_SST gradient (shown in Figs. 1a,b,d) thus dominate over the influence of the global SST trends outside the NIO and decrease the Indian monsoon rainfall. Over the Sahel, on the other hand, the effect of the weakening trend in the NIO\_SST gradient weakens the large Sahelian drying effect of the global SST trend outside of the NIO. From these experiments, we conclude that the observed weakening trend of the

NIO\_SST gradient is likely the major trigger for the decrease in the monsoon rainfall over India and has prevented the Sahel from getting too dry.

### 5. Role of the haze forcing

We next consider the relationship between the NIO\_SST gradient trend and the aerosol forcing. The INDOEX observations (Ramanathan et al. 2001) and a follow-on study (R2005) have shown that anthropogenic aerosols over South Asia and the NIO have decreased the surface solar radiation by as much as 7% from 1930 to 2000, while enhancing the lower-tropospheric (0–3 km) solar heating by about 30%–50%. By prescribing the observed SST trends we have implicitly accounted for the effects of the negative haze radiative forcing on the NIO SST. In addition, as shown earlier

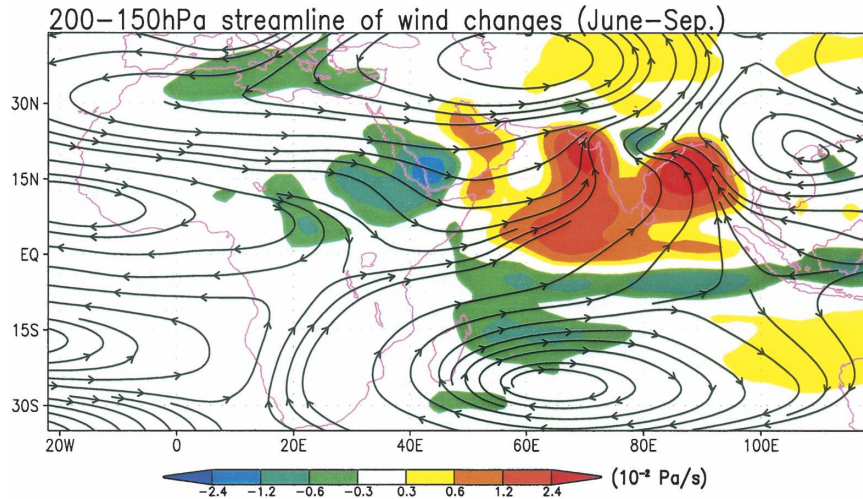


FIG. 4. Streamlines of the upper-troposphere wind change simulated by north Indian SST gradient change (IND – UNIF). Shading displays the simulated vertical motion change with red (blue) color associated with sinking (rising) motion at the 200–150-hPa level. Again, the vertical motion was calculated with pressure velocity  $\omega$  (in units of  $10^{-2} \text{ Pa s}^{-1}$ ).

(Chung and Ramanathan 2003), the solar heating of the troposphere by absorbing aerosols induces vertical motion locally over the domain of the brown haze and enhances rainfall locally. To assess this local effect of

aerosol solar heating, an additional experiment was conducted in which the brown haze radiative forcing was included in the model (HEAT1). Climatological SSTs were prescribed. As shown in Fig. 2d, the aerosol

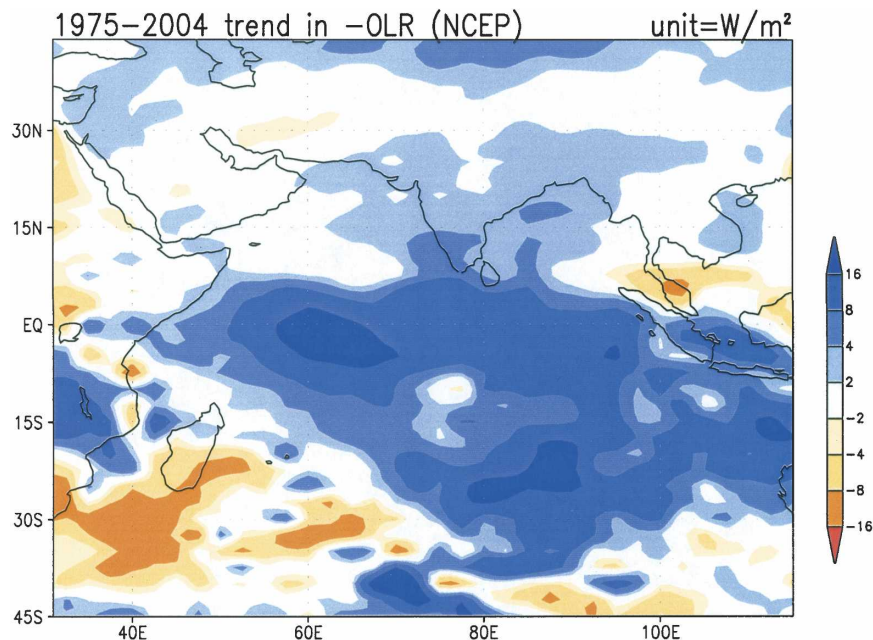


FIG. 5. The 1975–2004 trend in  $-1.0 \times \text{OLR}$  (negative of the outgoing longwave radiation) compiled by NOAA/Climate Prediction Center (CPC). Again, the trend values are in units of change over the entire trend period [and the trend unit  $(52 \text{ yr})^{-1}$  is omitted here], and a positive trend (blue color) indicates a decrease in OLR, i.e., an increase in cloud. The OLR data were downloaded from the IRI/LDEO Climate Data Library (<http://ingrid.ldeo.columbia.edu/>).



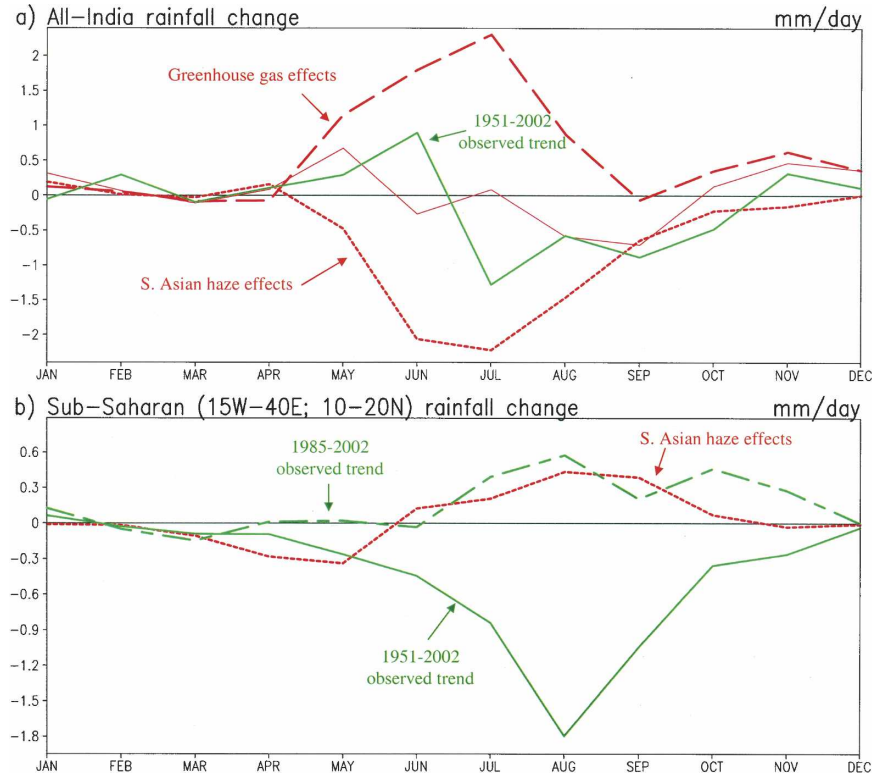


FIG. 6. Simulated and observed rainfall comparison. Green lines represent the observed trend in units of change over the entire period, and red lines the simulated change. The unit for the trend is  $[(\text{mm day}^{-1}) (52 \text{ yr})^{-1}]$ . For observation, we used the data from the Indian Institute of Tropical Meteorology (Parthasarathy et al. 1995) for (a) India, and we used the CRU dataset for (b) the African Sahel. The observed precipitation time series is found in Ramanathan et al. (2005) for India and Giannini et al. (2003) for the Sahel. For the red lines (simulated changes), the “greenhouse gas” effects represent the precipitation change by the hypothetical uniform warming in the NIO (UNIF – CONT), and the South Asian haze effects represent the precipitation change by the northern Indian SST gradient change + South Asian haze heating (IND – UNIF + HEAT1 – CONT). The thin red line in (a) is the sum of the two thick red lines. The simulated precipitation change has an uncertainty of about (a)  $0.2\text{--}0.3 \text{ mm day}^{-1}$  in summer and (b)  $0.1\text{--}0.2 \text{ mm day}^{-1}$  (95% confidence level).

tropospheric solar heating leads to excess rainfall over India and drought over sub-Saharan Africa, essentially opposing the precipitation changes due to the SST gradient reduction (Fig. 2c). The change in wind speed and vertical velocity also reveal (Fig. 3b) that the solar heating by absorbing aerosols provides a diabatic heating source for rising motion over NIO and India (Fig. 3b). However, the overall magnitude of the simulated precipitation change by the aerosol heating (Fig. 2d) is smaller than that due to the SST gradient change (Fig. 2c). Therefore, the net effect of the SST gradient change and the in situ haze heating (i.e., sum of Figs. 2c and 2d) is less rainfall over India and more rainfall over sub-Saharan Africa.

To obtain an overall perspective, the spatial average trends in monthly mean rainfall are shown for India (Fig. 6a) and sub-Saharan Africa (Fig. 6b). The ob-

served Indian summer (June–September) monsoon rainfall decreased from 1951 to 2002 by about  $0.5 \text{ mm day}^{-1}$  (Fig. 6a) with a peak decrease of about  $1.3 \text{ mm day}^{-1}$  during July. The uniform NIO\_SST warming trend (“GHGs effects”) and the weakening trend NIO\_SST gradient + haze heating (“haze effects”) lead to large competing rainfall changes from late spring to late summer with the rainfall changes peaking during July with respectively,  $+2$  and  $-2 \text{ mm day}^{-1}$ . These two competing effects combined (i.e., actual observed SST trend + haze heating) lead to weak drought (as shown by the thin red line in Fig. 6a). The implication is that aerosols, through their effects on the NIO\_SST gradients, have a strong drying effect on India. It is important to note that the relative cooling of the NIO (Fig. 1a) outweighs the direct effects of the haze forcing (i.e., haze atmosphere heating) in summer. During win-



ter and early spring, on the other hand, the haze forcing is much larger and dominates the circulation and regional hydrology over the effects of SST changes. Because of the ocean's large thermal inertia, the cooling of the NIO by the aerosols lags the aerosol radiative forcing by a few months. Thus while the increase in precipitation due to the local effect of the haze solar heating of the atmosphere is larger during spring (when the haze forcing is at its maximum; see Fig. 1d), the decrease in NIO\_SST gradient lasts well into summer and this delayed response creates a decrease in rainfall over India and an increase over sub-Saharan Africa in summer when the haze forcing is reduced. To test this hypothesis, we increased the haze radiative forcing during summer to its peak value during early spring (a three- to fourfold increase in the haze summer forcing) in another experiment (HEAT2), and the increase in Indian summer rainfall (up to  $3.5 \text{ mm day}^{-1}$ ; HEAT2 – CONT) exceeded the decrease (up to  $-2.5 \text{ mm day}^{-1}$ ) due to the weakening NIO\_SST gradient (IND – UNIF).

The observed June–September rainfall decrease in the Sahel from 1951 to 2002 is about  $1.0 \text{ mm day}^{-1}$ . The drying trend peaks in August (Fig. 6b). Also shown in this figure is the rainfall trend after 1985, which shows a positive rainfall trend of about  $0.3$  to  $0.6 \text{ mm day}^{-1}$  during summer. The rainfall increase driven by the NIO\_SST gradient trend during this period is about  $0.5 \text{ mm day}^{-1}$ , and the increase by the overall haze effects (i.e., haze heating and SST gradient change) is about  $0.3 \text{ mm day}^{-1}$  (red line in Fig. 6b). Compared to the observed drying trend, the model simulations suggest that the South Asian haze has mitigated the Sahel desiccation considerably. As a supporting point, we note that the black carbon emission in India has doubled from the early 1980s to the late 1990s (Novakov et al. 2003), coinciding with the period when the Sahelian drought abated (Fig. 6b).

## 6. Implications

We have presented evidence from observations that the equatorial Indian Ocean has warmed by about  $0.6$  to  $0.8 \text{ K}$  during 1950 to 2002, accompanied by a dramatic weakening of the summertime SST gradient in the NIO. In the model the weakening of the meridional NIO\_SST gradient leads to a large decrease in Indian rainfall during summer months, ranging from  $2$  to  $3 \text{ mm day}^{-1}$ . Reduction in the NIO\_SST gradient basically weakens the model monsoonal circulation and shifts model rainfall from India to sub-Saharan Africa. This raises the possibility that the recovery of the Sahelian drought since the 1980s may in part be due to the weak-

ening of the Indian Ocean SST gradient. While we do not rule out the role of natural factors (such as Indian Ocean dipole and ENSO) in the observed SST trends, we used published climate model simulations in conjunction with the findings of this study in an attempt to link the observed SST trends and rainfall to anthropogenic forcing terms.

GHGs by themselves lead to large positive anomalies in the simulated Indian rainfall, which leads to the speculation that, when the South Asian aerosol pollution is cut down significantly, India may witness a large increase ( $10\%$ – $20\%$ ) in monsoon rainfall. The direct effect of aerosol solar heating of the atmosphere acts as an important positive forcing for the monsoonal circulation. One implication of this solar heating is that variations in aerosol pollution can lead to large interannual and intraseasonal variability in rainfall. Indeed, satellite and ground-based aerosol observations (Li and Ramanathan 2002) reveal large (as much as  $25\%$  with an extreme of  $50\%$ ) interannual variations in winter and summer aerosol concentrations. One scenario is that a failure of monsoon in one summer month can lead to dry conditions with enhanced dust and other man-made aerosol loading (Sikka 2003), which can in turn lead to more rainfall during the following month. Such interactions and feedbacks between monsoon rainfall and aerosol loading can contribute to intraseasonal and interannual variability.

**Acknowledgments.** This work was initiated when V. Ramanathan was visiting the National Center for Atmospheric Research. Dr. Jim Hurrell's work on African rainfall helped motivate the African rainfall part of this study and we thank him for stimulating discussions. We thank Fang Li of Scripps Institution of Oceanography for help with data handling. This work was supported by NASA (NNG04GC58G) and NSF (ATM-0201946).

## REFERENCES

- Bonan, G. B., 1996: A land surface model (LSM version 1.0) for ecological, hydrological, and atmospheric studies: Technical description and user's guide. NCAR Tech. Rep. TN-417+STR, 122 pp.
- Chung, C. E., and V. Ramanathan, 2003: South Asian haze forcing: Remote impacts with implications to ENSO and AO. *J. Climate*, **16**, 1791–1806.
- , —, and J. T. Kiehl, 2002: Effects of the South Asian absorbing haze on the Northeast monsoon and surface–air heat exchange. *J. Climate*, **15**, 2462–2476.
- Douville, H., J. F. Royer, J. Polcher, P. Cox, N. Gedney, D. B. Stephenson, and P. J. Valdes, 2000: Impact of  $\text{CO}_2$  doubling on the Asian summer monsoon: Robust versus model-dependent responses. *J. Meteor. Soc. Japan*, **78**, 421–439.
- Giannini, A., R. Saravanan, and P. Chang, 2003: Oceanic forcing

- of Sahel rainfall on interannual to interdecadal time scales. *Science*, **302**, 1027–1030.
- Hoerling, M. P., J. W. Hurrell, and J. Eischeid, 2006: Detection and attribution of twentieth-century northern and southern African rainfall change. *J. Climate*, in press.
- Hulme, M., 1996: Recent climatic change in the world's drylands. *Geophys. Res. Lett.*, **23**, 61–64.
- Kaplan, A., M. Cane, Y. Kushnir, A. Clement, M. Blumenthal, and B. Rajagopalan, 1998: Analyses of global sea surface temperature 1856–1991. *J. Geophys. Res.*, **103**, 18 567–18 589.
- Kaufman, Y. J., D. Tanré, and O. Boucher, 2002: A satellite view of aerosols in the climate system. *Nature*, **419**, 215–223.
- Kiehl, J. T., J. J. Hack, G. B. Bonan, B. A. Boville, D. L. Williamson, and P. J. Rasch, 1998: The National Center for Atmospheric Research Community Climate Model: CCM3. *J. Climate*, **11**, 1131–1149.
- Li, F., and V. Ramanathan, 2002: Winter to summer monsoon variation of aerosol optical depth over the tropical Indian Ocean. *J. Geophys. Res.*, **107**, 4284, doi:10.1029/2001JD000949.
- May, W., 2002: Simulated changes of the Indian summer monsoon under enhanced greenhouse gas conditions in a global time-slice experiment. *Geophys. Res. Lett.*, **29**, 1118, doi:10.1029/2001GL013808.
- Meehl, G. A., and J. M. Arblaster, 2003: Mechanisms for projected future changes in south Asian monsoon precipitation. *Climate Dyn.*, **21**, 659–675.
- , P. Gent, J. M. Arblaster, B. Otto-Bliesner, E. Brady, and A. Craig, 1993: South Asian summer monsoon variability in a model with doubled atmospheric carbon dioxide concentration. *Science*, **260**, 1101–1104.
- Mitchell, T. D., and P. D. Jones, 2005: An improved method of constructing a database of monthly climate observations and associated high-resolution grids. *Int. J. Climatol.*, **25**, 693–712.
- Novakov, T., V. Ramanathan, J. E. Hansen, T. W. Kirchstetter, M. Sato, J. E. Sinton, and J. A. Satoh, 2003: Large historical changes of fossil-fuel black carbon aerosols. *Geophys. Res. Lett.*, **30**, 1324, doi:10.1029/2002GL016345.
- Parthasarathy, B., A. A. Munot, and D. R. Kothawale, 1995: Monthly and seasonal rainfall series for all-India homogeneous regions and meteorological subdivisions: 1871–1994. IITM Research Rep. 065, Pune, India, 10 pp.
- Ramanathan, V., 1981: The role of ocean–atmosphere interactions in the CO<sub>2</sub>–climate problems. *J. Atmos. Sci.*, **38**, 918–930.
- , and Coauthors, 2001: The Indian Ocean Experiment: An integrated analysis of the climate forcing and effects of the Great Indo-Asian Haze. *J. Geophys. Res.*, **106**, 28 371–28 398.
- , and Coauthors, 2005: Atmospheric brown clouds: Impacts on South Asian climate and hydrological cycle. *Proc. Natl. Acad. Sci. USA*, **102**, 5326–5333.
- Rayner, N. A., D. E. Parker, E. B. Horton, C. K. Folland, L. V. Alexander, D. P. Rowell, E. C. Kent, and A. Kaplan, 2003: Global analyses of sea surface temperature, sea ice, and night marine air temperature since the late nineteenth century. *J. Geophys. Res.*, **108**, 4407, doi:10.1029/2002JD002670.
- Rotstayn, L. D., and U. Lohmann, 2002: Tropical rainfall trends and the indirect aerosol effect. *J. Climate*, **15**, 2103–2116.
- Sikka, D. R., 2003: Evaluation of monitoring and forecasting of summer monsoon over India and a review of monsoon drought of 2002. *Proc. Indian Natl. Sci. Acad.*, **69**, 479–504.
- Smith, T. M., and R. W. Reynolds, 2004: Improved extended reconstruction of SST (1854–1997). *J. Climate*, **17**, 2466–2477.
- Webster, P. J., and J. Fasullo, 2003: Monsoon: Dynamical theory. *Encyclopedia of Atmospheric Sciences*, J. Holton and J. A. Curry, Eds., Academic Press, 1370–1386.
- , V. O. Magana, T. N. Palmer, J. Shukla, R. A. Tomas, M. Yanai, and T. Yasunari, 1998: Monsoons: Processes, predictability, and the prospects for prediction. *J. Geophys. Res.*, **103**, 14 451–14 510.